Spatiotemporal patterns and symmetry breaking on a ring electrode

B. J. Green and J. L. Hudson
Department of Chemical Engineering, University of Virginia, 102 Engineers' Way, Charlottesville, Virginia 22904-4741
(Received 28 August 2000; published 25 January 2001)

A series of experiments on a ring electrode with changes in a parameter, the applied potential, are described. Spatiotemporal patterns are investigated in a region of parameter space in which relaxation oscillations occur. The simplest state is a period 2Π oscillation that has full O(2) symmetry so that at each instant the pattern is unchanged by rotations or reflections of the ring. With change in parameter a spatiotemporal period doubling occurs to period 4Π. This is followed by a symmetry breaking to another state with period 4Π and subsequently by a second period doubling to period 8Π. Proper orthogonal decomposition is used as an aid in elucidating the nature of the transitions.

DOI: 10.1103/PhysRevE.63.026214 PACS number(s): 82.40.Bj, 82.45.−h

I. INTRODUCTION

Spatiotemporal patterns have been observed and analyzed in a variety of chemically reacting systems [1], including combustion [2,3], gas-solid reactions [4–6], and liquid phase reactions [7–11]. Numerous examples are now known in bistable, excitable and oscillatory media including fronts, waves, Turning patterns, spiral waves, and breakup into turbulence.

Electrochemical reactions in particular are known to exhibit temporal oscillations, bistability, and excitability [12] as well as spatiotemporal patterns [13]. The patterns are commonly produced by a combination of nonlinear reaction kinetics and potential drop through the electrolyte; the coupling mechanisms have been discussed in detail in some recent papers [13–17]. A ring geometry has been used in many of the studies to produce a variety of controlled patterns including rotating waves [18] and standing waves [16].

The results described here were obtained during the electrodissolution of iron in sulfuric acid. This reaction system has been used by several investigators to study pattern formation in two disparate regions of parameter space. In one of these, higher frequency—often chaotic—oscillations arise [19]. In the other region of parameter space, much slower relaxation oscillations occur and it is in this region that the spatiotemporal patterns discussed in this paper arise. Pigeaud and Kirkpatrick carried out an early investigation of one type of pattern on a disk surface, viz., waves with approximate O(2) symmetry during period 1 oscillations [20]. These studies were subsequently extended to other patterns on both disk and ring geometries [21,22].

We present here additional results obtained with the iron system on a ring geometry and thus add to the library of types of pattern and symmetry breaking bifurcation observed in reacting systems. With the aid of video images and decomposition of patterns by Karhunen-Loève expansions, we show how an oscillatory pattern with O(2) symmetry undergoes a spatiotemporal period doubling, another symmetry breaking, and finally a subsequent second period doubling into a period 4 state.

II. EXPERIMENTS

A standard three-electrode electrochemical cell (working electrode, counterelectrode, and reference electrode) is used. The working electrode is an iron ring (cut from a 99.9985% iron rod, Aesar Puratronic) with outside diameter of 12 mm and inside diameter of 6 mm and encased in epoxy so that only the annular shaped face is exposed. The total surface area of the electrode is 84.82 mm^2 and the diameter of the epoxy is 33 mm. The ring is placed in a solution of 1*M* H_2SO_4 and 1*M* Na_2SO_4 approximately 2–3 cm below the surface of the liquid. There is no stirring and the fluid is nearly stagnant. All experiments were performed at ambient temperature.

A platinum foil counterelectrode arranged in a circle with a 12 cm diameter is used for the cathodic reaction. It is in the horizontal plane of the working electrode. The reference electrode is Hg/Hg_2SO_4 and its tip is placed in the horizontal plane of the working electrode, just outside the radius of the epoxy. The control parameter is the applied potential; it is controlled by a PAR EG&G model 273 potentiostat.

Polarized light is shone on the iron surface and the images

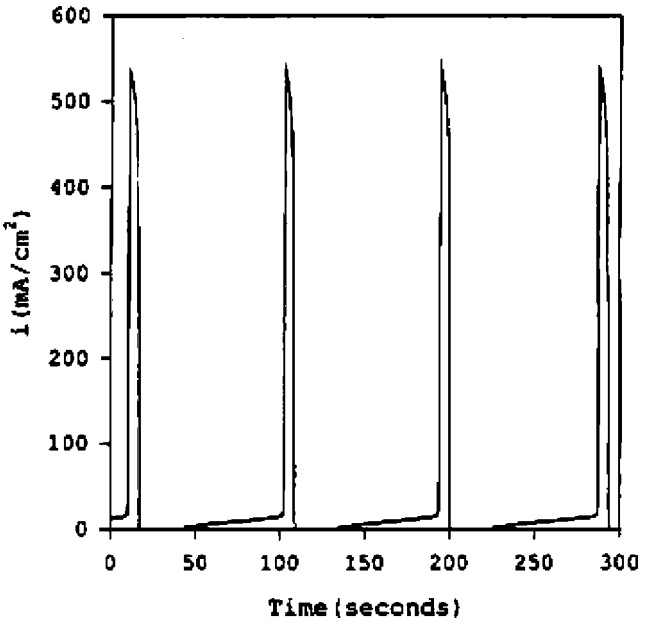

FIG. 1. A time series of the current for an iron ring undergoing electrodissolution at potentiostatic conditions. The pattern is formed during the passivation phase of the cycle.

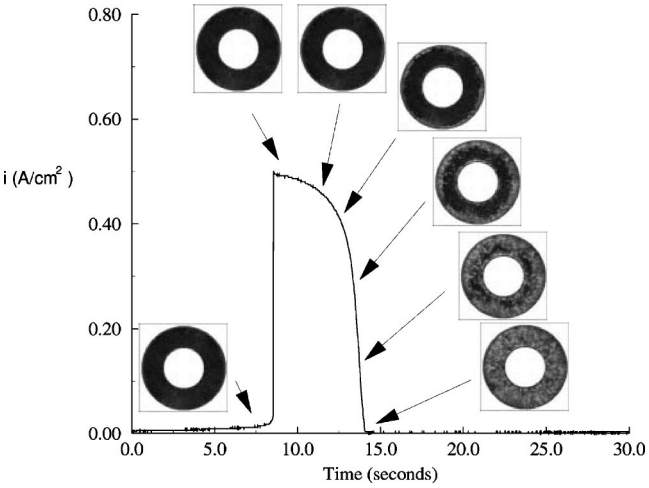

FIG. 2. Period 1 oscillations. Snapshots of the spatiotemporal pattern that forms on the iron ring electrode surface. The pattern is formed during the passivation as waves move from the inner and outer radii of the ring. The pattern exhibits full O(2) symmetry. Snapshots from 7 to 17 s are used in the image decomposition analysis. Applied potential is −158 mV.

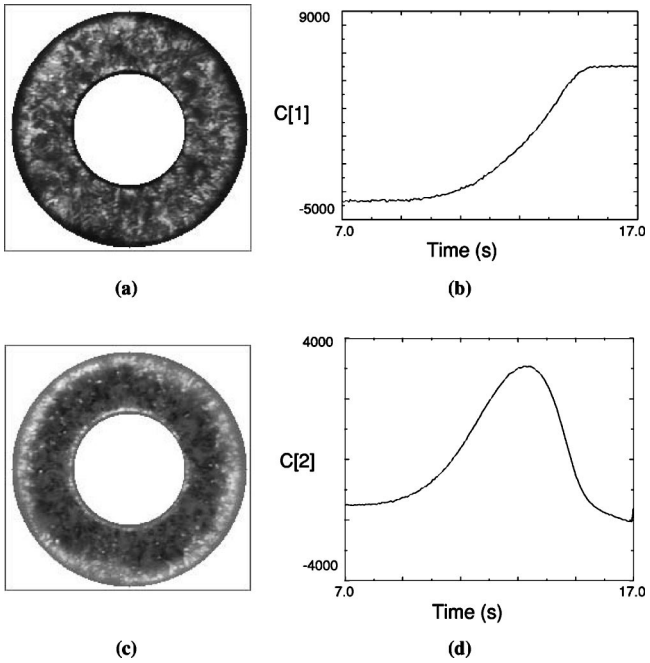

FIG. 3. Decomposition of the period 1 oscillation. Applied potential −158 mV. (a) First mode; (b) first coefficient; (c) second mode; (d) second coefficient.

are recorded using a JVC S-VHS video camera with a cross-polarized lens and VCR. The recorded images were digitized and manipulated using an SGI workstation.

III. RESULTS

All the experiments are carried out in a parameter region in which slow, active-passive relaxation oscillations occur. An example of a time series of the total current from the ring is shown in Fig. 1. (The amplitude and period both depend on applied potential; the period decreases with decreasing potential.) The total signal is near zero for an extended time, begins to rise slowly, and then undergoes a rapid rise during the activation of the surface, followed by a somewhat slower decrease back to near zero during the passivation phase. Most of the pattern formation to be discussed occurs during this passivation phase.

We will present here a series of five types of behavior that occur as the parameter, the applied potential, is altered. Images of the behavior are shown at instants in time at each of the five values of the parameter. The images are those obtained directly from the experiments and have not been filtered or otherwise altered. The activation and passivation can be seen from the black/white coloration as follows: Consider one activation/passivation cycle corresponding to a single rise and fall of the current in Fig. 1. Start in the passive state where the surface appears black through the cross-polarized

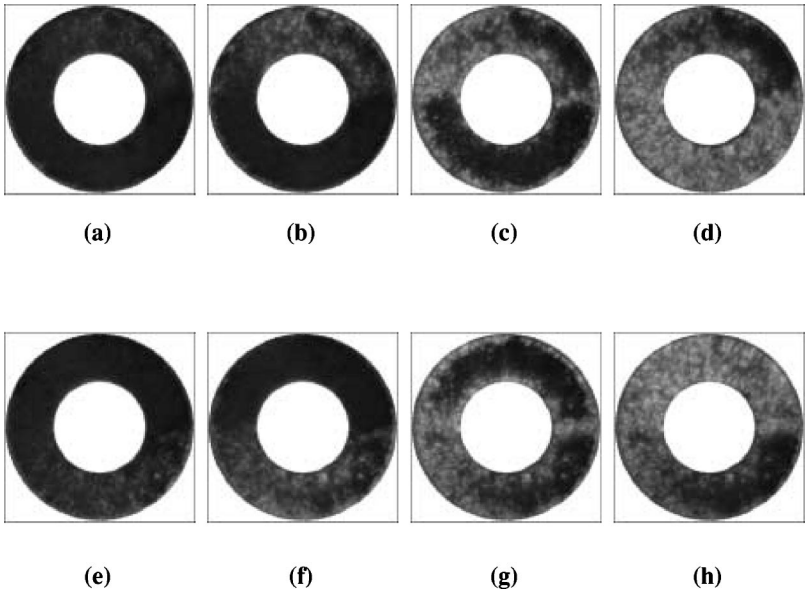

FIG. 4. Snapshots of the pattern from a period 2 oscillation. (a)–(d) pattern during the first passivation; (e)–(h) pattern during the second passivation. Parts (e)–(h) are equivalent to parts (a)–(d) when reflected about the horizontal axis. Applied potential is −163 mV.

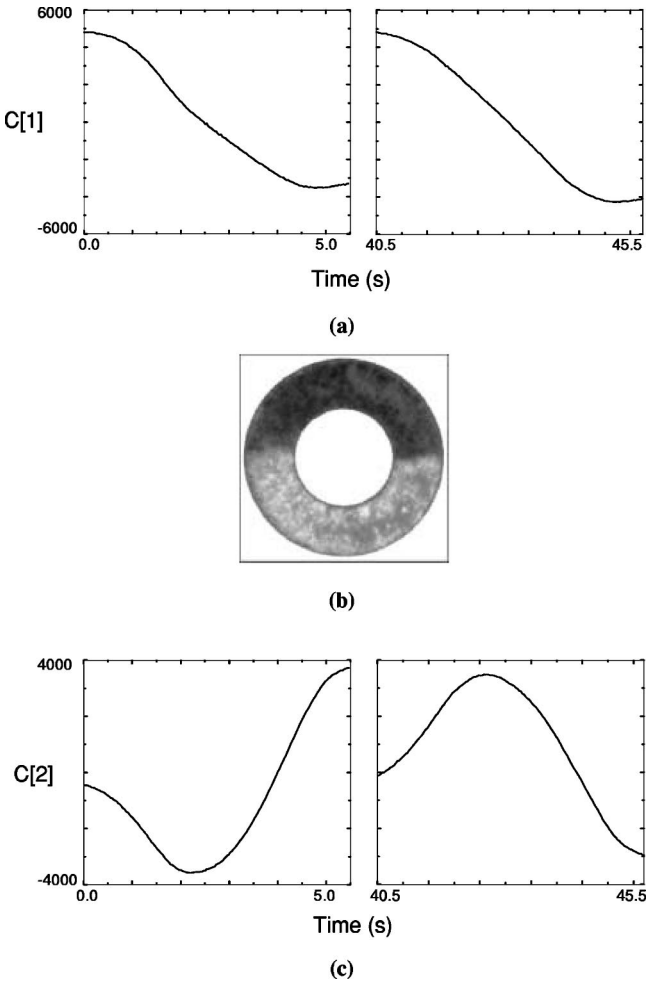

FIG. 5. Period 2 oscillation: eigenfunctions and coefficients. (a) Coefficient of the first eigenfunction during the first and second passivation sequences; the eigenfunction (not shown) is uniform. (b) Second eigenfunction. (c) Coefficient of second eigenfunction during the first and second passivation sequences.

lighting. The surface activates with no visible change. (The activation is faster than the 30 Hz frequency of the video camera.) As a passivation wave covers the surface a colloid is produced which appears white and produces the patterns shown. As the colloid slowly dissolves the image appears darker and eventually returns to black before the next activation-passivation sequence.

In the next five subsections we shall see a sequence of patterns the first of which has O(2) symmetry; symmetry breakings then occur with changes in the parameter. There are, however, heterogeneities on the electrode surface and so none of the patterns is perfect. For example, consider the patterns in Figs. 2 and 3 below that we state have O(2) symmetry. By that we mean that the pattern is O(2) with noise. The heterogeneities, however, do not seem to affect the dynamics or the intrinsic nature of the patterns. We have, for example used several different rings of different sizes and have obtained the same sequence of patterns. We have also rotated a given ring between experiments, that is, carried out an experiment, rotated the ring, and done the experiment again; the results were not affected.

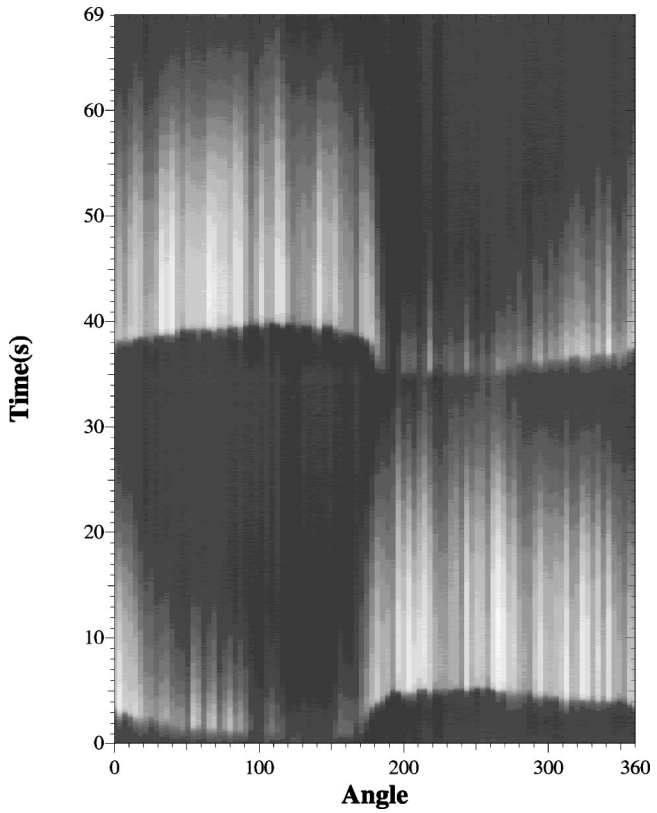

FIG. 6. Period 2 oscillation. Pattern on a thin ring for a 69 s interval (one full period). Applied potential is −163 mV.

A. Period 1 oscillations: $V_0 = -158$ mV

In Fig. 2 the activation/passivation portion of a single cycle is shown on an expanded time scale. Images corresponding to one instant before the activation and six times

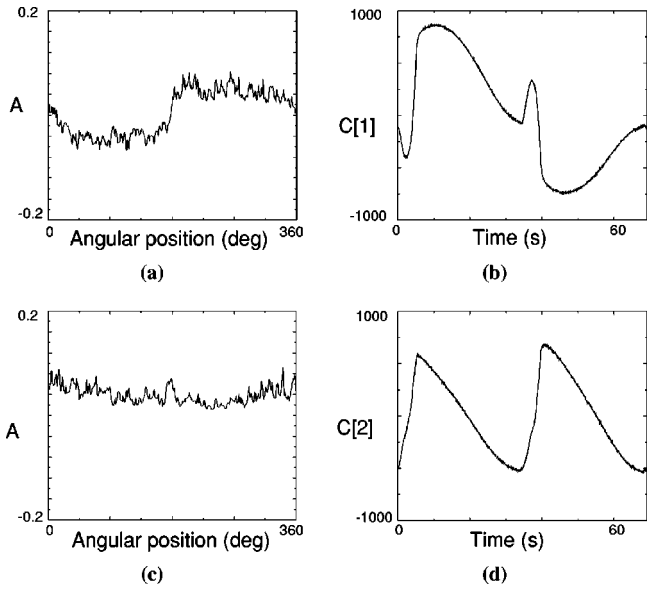

FIG. 7. Period 2 oscillation. Decomposition of snapshots of the thin ring corresponding to Fig. 6. (a) First mode; (b) first coefficient; (c) second mode; (d) second coefficient. Applied potential is −163 mV.

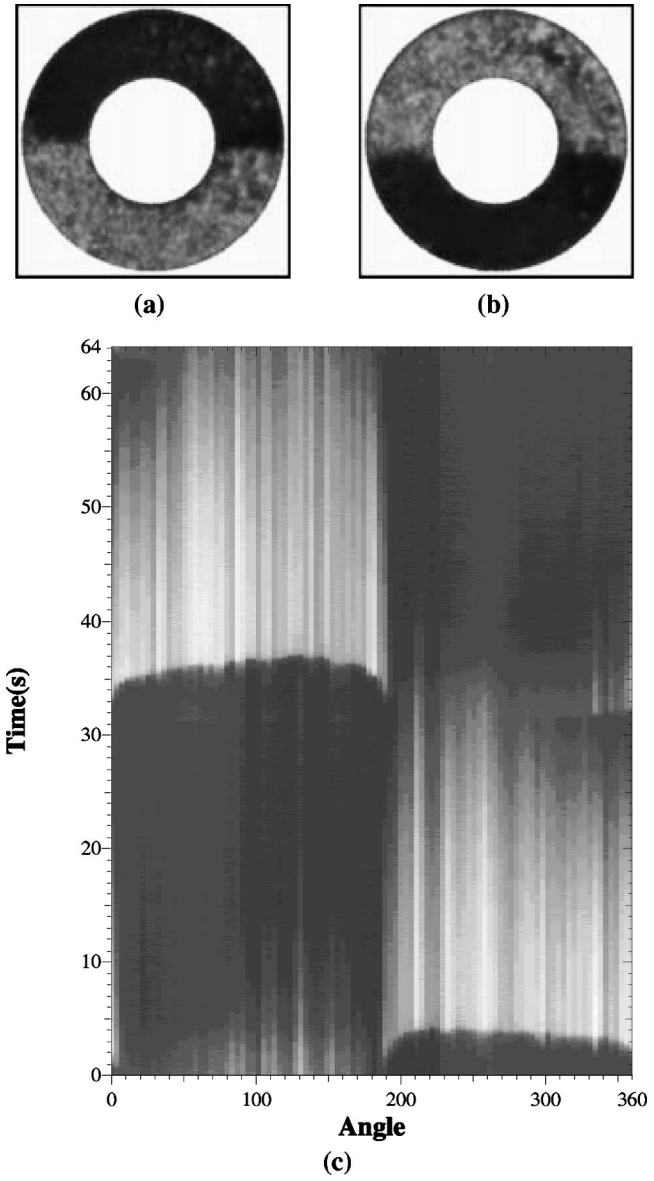

FIG. 8. Period 2 antiphase oscillations. (a) Snapshot of the pattern near the end of the first passivation sequence. (b) Snapshot of the pattern near the end of the second passivation sequence. (c) Behavior on a thin ring for a 64 s interval (one full period). Applied potential is −164.5 mV.

during the passivation are shown. A wave progresses from the outer radius of the ring inward and, in addition, a second wave starts after a time delay at the inner radius and moves outward, until it meets the first front. There is a full O(2) symmetry; at each instant the pattern is unchanged by rotations or reflections of the ring [23]. The state is a periodic solution p_1 with a period that we define as 2Π. The radial dependency is not essential to the behavior being investigated. In discussion of later states we shall take a thin ring from the finite thickness ring and investigate its behavior in order to show the type of transition occurring. Obviously the thin ring exhibits no radial dependence and therefore its behavior depends only on time under the conditions of Fig. 2 where there is no angular variation. The temporal variation is periodic with period 2Π.

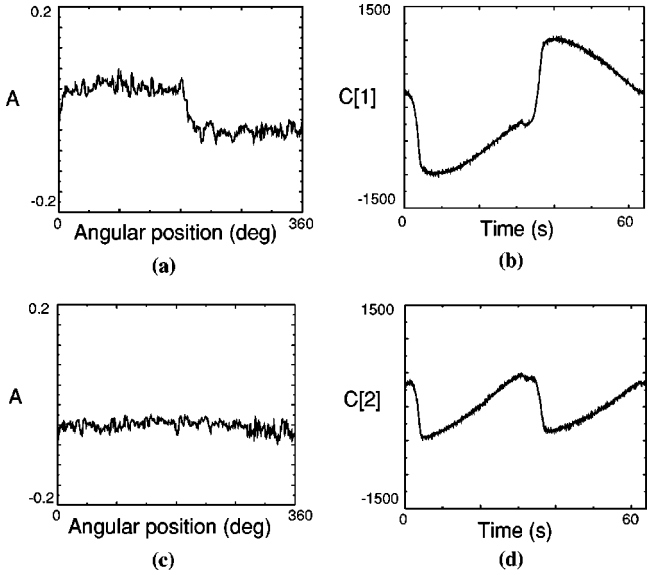

FIG. 9. Period 2 antiphase oscillations. Decomposition of the thin ring corresponding to Fig. 8. (a) First mode; (b) first coefficient; (c) second mode; (d) second coefficient. Applied potential is −164.5 mV.

A proper orthogonal decomposition (Karhunen-Loève expansion) [24,25] has been made of all the states investigated, both of the full (nonzero thickness) ring and of the thin slice. Although the behavior of the state being discussed in this section is simple and can be well characterized without resorting to any decomposition, we do present some information on the decomposition as it will be useful as a comparison to later states. The first two modes and coefficients from the full ring decomposition are shown in Fig. 3; the cumulative normalized energies using one and two modes are 76% and 91%, respectively. One mode captures the uniform periodic behavior and the second mode adds the radially dependent component. Note that the time over which the coefficients are shown is not that of the entire period, but rather only that portion during which the pattern changes significantly with time, that is, during the activation/passivation portion of the cycle. The time scale of Fig. 3 corresponds to that of Fig. 2. A decomposition of the thin ring can of course be made with a single mode; the first mode then contains 90% of the normalized energy with the deviation from 100% due to heterogeneities of the surface and noise in the data.

B. Period 2 oscillations: $V_0 = -163$ mV

A series of snapshots of the behavior at a somewhat lower value of the parameter is shown in Fig. 4. The period has now doubled to 4Π and extends over two activation/passivation cycles of a time series such as that seen in Fig. 1. The images on the first half of the complete cycle are shown in Figs. 4(a)–4(d) and those on the second half in Figs. 4(e)–4(h). Again, as in the previous section, all these images are from the activation/passivation portion of the cycle. Note that the passivation begins at the top of the ring in the first half cycle and proceeds to the bottom. In the second half cycle the passivation begins at the bottom and proceeds to

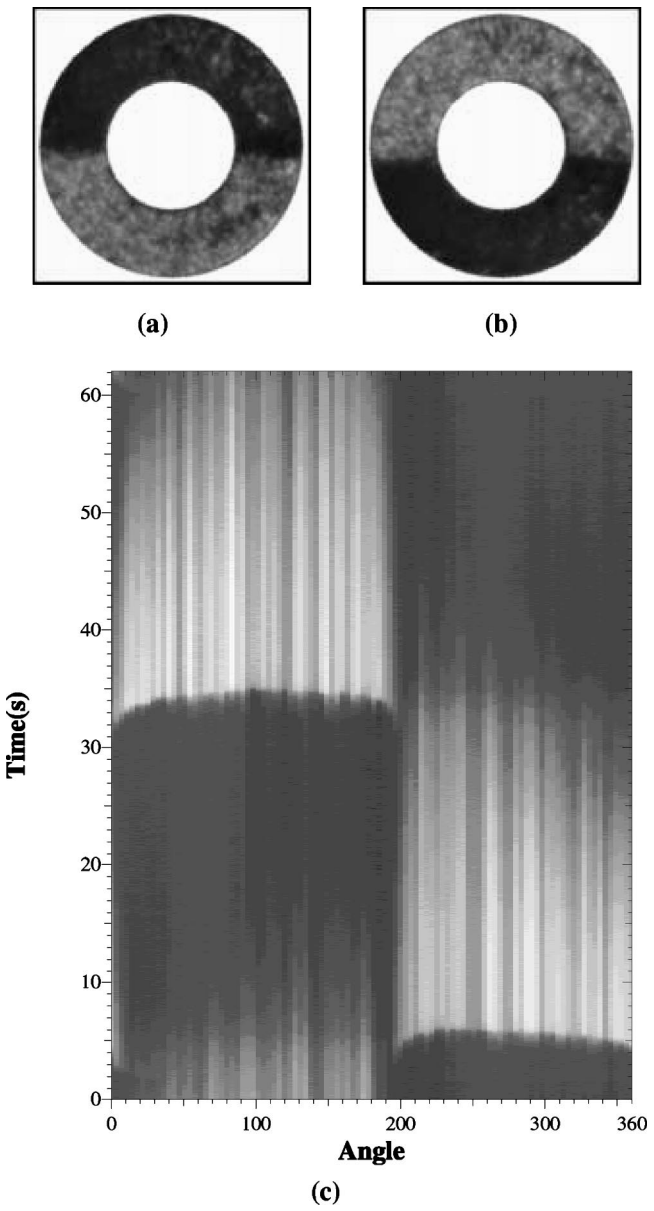

FIG. 10. Symmetry broken period 2 oscillation. (a) Snapshot of final pattern of first passivation sequence. (b) Snapshot of final pattern of second passivation sequence. (c) Space-time plot of thin ring during a 62 s interval (one full period). Applied potential is −165 mV.

the top. It does not appear that the pattern can be reflected about the vertical axis; that is, the vertical axis does not appear to be a line of symmetry. Note, for example, that the dark portion of the pattern in Figs. 4(c) and 4(d) and again in Figs. 4(g) and 4(h) lies to the right of the vertical axis. A reflection of the pattern about the horizontal axis (but not a rotation of the pattern by 180°) is equivalent to a half-period phase shift.

The orientation of the patterns in Fig. 4 and in subsequent similar figures does depend on the geometry of the apparatus; for example, changing the angular position of the reference electrode (without changing the counterelectrode, which is a circle surrounding the ring working electrode)

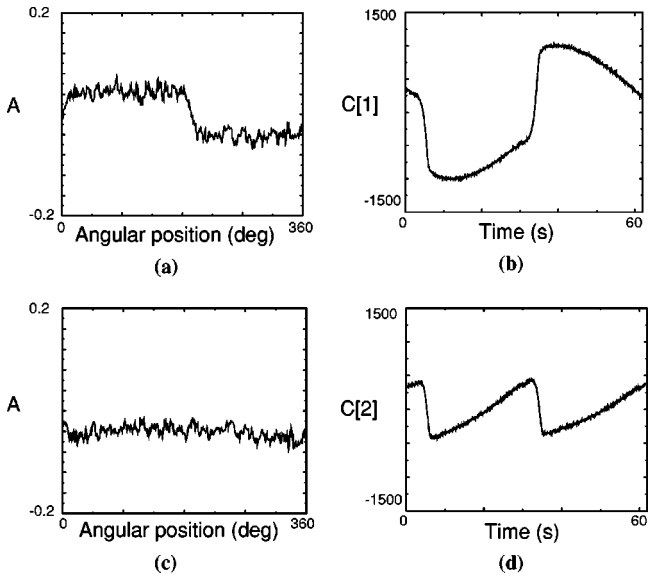

FIG. 11. Decomposition of the thin ring during the symmetry broken period 2 oscillation. (a) First mode; (b) first coefficient; (c) second mode; (d) second coefficient. Applied potential is −165 mV.

does rotate the patterns. In presenting the results we rotate the patterns so that the series of results can be compared within itself.

Proper orthogonal decomposition (POD) modes and coefficients are shown in Fig. 5. The first eigenfunction is almost uniform and is not shown. The first two modes capture 78% of the normalized energy; higher modes are required to reconstruct the azimuthal motion of the pattern. As noted above, most of the important features of the spatiotemporal patterns can be seen without recourse to the radial dependence and we therefore made a thin circular slice through the data. The temporal behavior of one slice is shown as a space (angle) vs time plot in Fig. 6. Note that the behavior is shown for a longer time than in Figs. 4 and 5; an entire period, including the long time in which the electrode is essentially passive, is seen here. The first two eigenmodes and coefficients from a decomposition of the one-dimensional slice are shown in Fig. 7. These two modes capture 93% of the cumulative normalized energy and can be used to reconstruct the essential features of the one-dimensional dynamics.

C. Period 2 antiphase oscillations: $V_0 = -164.5$ mV

Two snapshots of the conditions at the end of two successive passivations are presented in Figs. 8(a) and 8(b). This state differs from that shown immediately above in its symmetries. In the present state either a rotation by 180° or a reflection about the horizontal axis is equivalent to a half-period phase shift. Furthermore, there is a line of symmetry, i.e., the pattern can be reflected about the vertical axis.

The pattern on the thin ring can be seen in the space-time plot of Fig. 8(c). The first two modes and coefficients of the decomposition are shown in Fig. 9. The cumulative normalized energy of the two modes is 94%. The second mode is uniform and its coefficient has period 2Π. The coefficient of

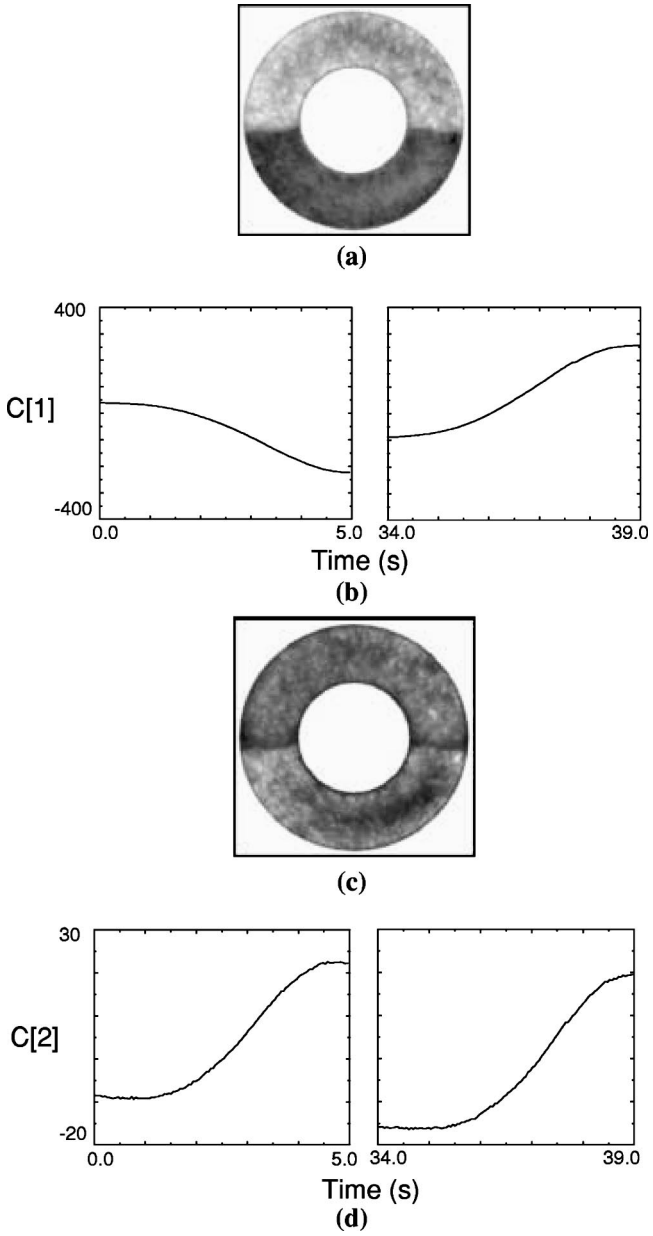

FIG. 12. Decomposition of the full ring images during the symmetry broken period 2 oscillation. (a) First mode. (b) First coefficient during the first and second passivations. (c) Second mode. (d) Second coefficient during the first and second passivations.

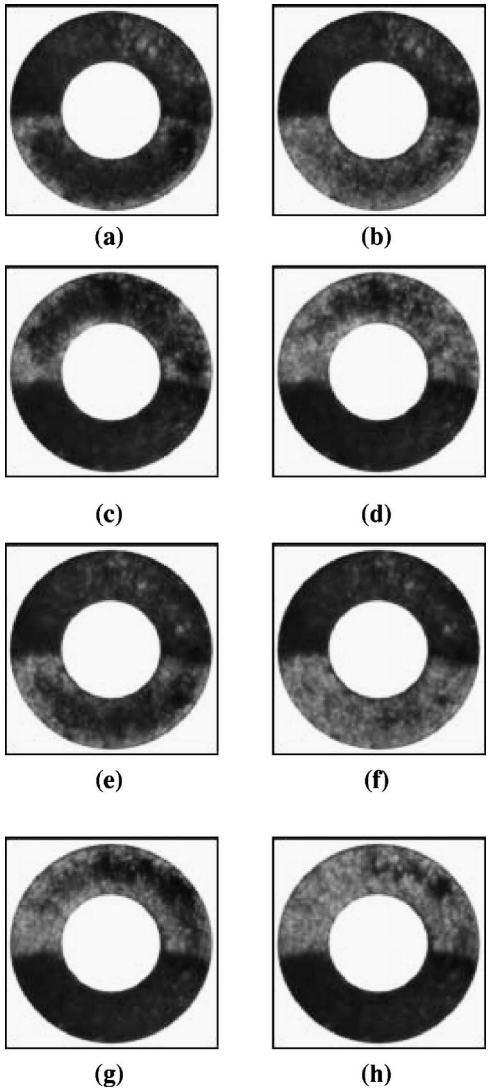

FIG. 13. Period 4 oscillation. Snapshots during (a), (b) the first passivation, (c), (d) the second passivation, (e), (f) the third passivation, and (g), (h) the fourth passivation. Applied potential is −165.5 mV.

the first mode, however, has period 4Π. The essential features of the overall pattern and symmetries can be reconstructed with the two modes.

D. Symmetry broken period 2 oscillations: $V_0 = -165$ mV

As the potential is lowered further, symmetries seen in the preceding state are broken. This can be seen in Figs. 10 and 11, which correspond to Figs. 8 and 9 above. Note in the snapshots Figs. 10(a) and 10(b) that there is again a vertical line of symmetry. However, neither a reflection about the horizontal axis nor a rotation by 180° is equivalent to a half-period phase shift. Symmetry has been broken. This can perhaps most clearly be seen in the space-time plot made from the one-dimensional circular slice [Fig. 10(c)] and its decomposition (Fig. 11). Note now in Fig. 10(c) that the pattern is not symmetrical about 180° with a shift of a half period but rather the ring is broken into two segments of approximately 190° and 170°; this can be contrasted with the previous behavior seen in Fig. 8(c). The first two modes and coefficients of the decomposition of the one-dimensional slice are shown in Fig. 11; they differ from those of Fig. 9 only in the first eigenfunction where the division into (approximately) 190° and 170° segments can be seen.

Results from the decomposition of the entire ring are shown in Fig. 12. Although the characteristics of this state and the transitions to it can already be ascertained from Figs. 10 and 11, we present this decomposition for the full ring data so that it can be used as a basis for the discussion of the transition to the next state in the next section. The first eigenfunction is shown in Fig. 12(a). It does have a line of symmetry, the vertical axis; however, the top (light) region ex-

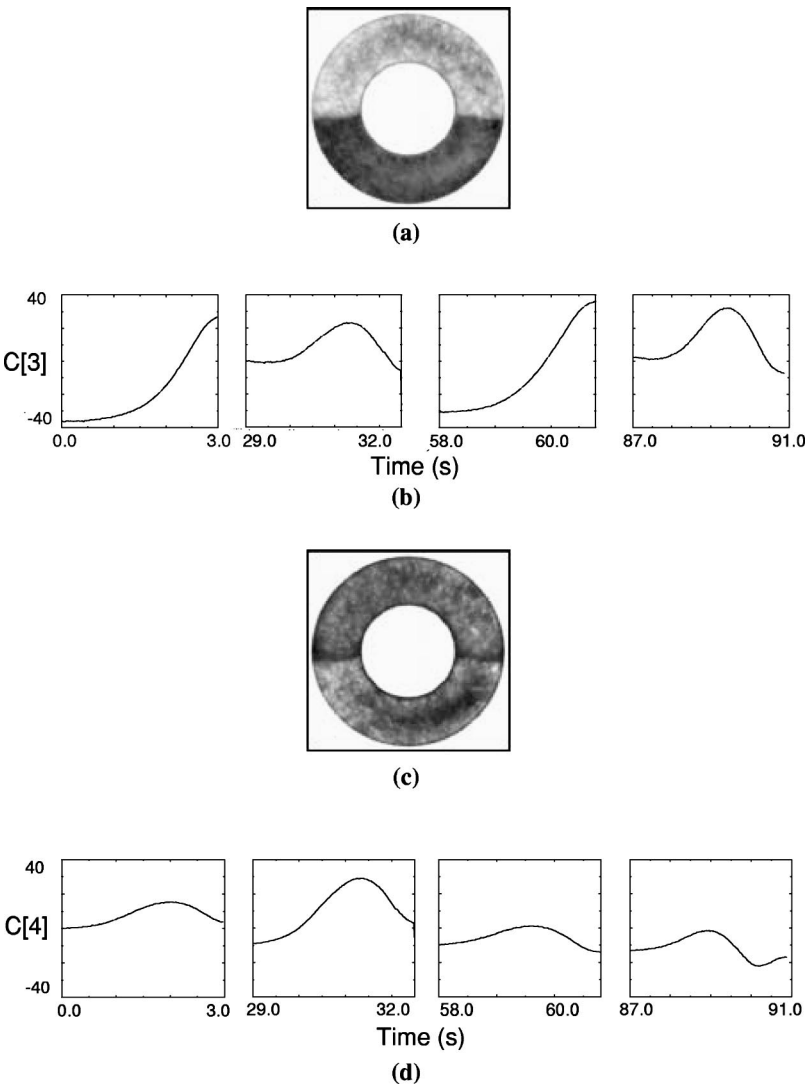

FIG. 14. Decomposition of period 4 oscillation. (a) Third mode. (b) Third coefficient during four passivation sequences. (c) Fourth mode. (d) Fourth coefficient during four passivation sequences.

tends somewhat below the horizontal axis. The coefficient of the first eigenfunction is seen in Fig. 12(b) for the first and second passivations. The second eigenfunction is uniform and is not shown. The coefficient for the second eigenfunction is shown in Fig. 12(c) for the two passivations corresponding to those seen in Fig. 12(b).

Thus we see that the behavior of the patterns in this section and in the previous one both have period 2, i.e., have a period of 4π. However, in the second p_2 state, a symmetry has been broken in that a rotation by 180° is no longer equivalent to a half-period phase shift. As discussed by Swift and Wiesenfeld [26] and by Fiedler [27], such a symmetry breaking makes possible a subsequent period doubling such as that which we shall see in the next section. For related results involving chemical oscillators see, for example, Ref. [28].

E. Period 4 oscillations: $V_0 = -165.5$ mV

After the symmetry breaking of the period 2 state, a second period doubling occurs. The resulting state is then p_4 or, equivalently, has period 8π. In relation to Fig. 1, a complete cycle now requires four activation/passivation cycles and thus four maxima of the time series.

Snapshots from the period 4 oscillations are shown in Fig. 13. Two snapshots from each of the four cycles are given with (a), (b) the first cycle, (c), (d) the second, etc. The period doubling to the period 8π state occurs through a loss of symmetry about the vertical axis. Note, for example, Figs. 13(d) and 13(h), which represent states near the end of the second and fourth activation/passivation cycles, respectively. In Fig. 13(h) it can be seen that the passivation is not yet complete in a region offset from the vertical axis, that is, at a location at approximately 45°.

A decomposition has also been carried out on these data and can be used to distinguish the behavior from that shown in the preceding section and to ascertain the nature of the period doubling. Four terms of the expansion are required to reproduce the qualitative features of the dynamics. The first two eigenfunctions and their coefficients are the same as those obtained before the period doubling, i.e., they are the same as those shown in Fig. 12. (Therefore, they are not shown again here.) The third and fourth eigenfunctions are presented in Figs. 14(a) and 14(c), respectively; the coeffi-

cients can be seen in Figs. 14(b) and 14(d) for the four consecutive activation/passivation cycles making up the entire 8π period. The fourth eigenfunction [Fig. 14(c)] does not have a vertical line of symmetry; the period 4 nature of the oscillations can be seen in the coefficient [Fig. 14(d)], i.e., the period of this coefficient is 8π.

IV. FINAL COMMENTS

An anodic reaction, the electrodissolution of a metal, has been carried out on a ring electrode in the oscillatory regime. During the oscillations films grow and recede, thus producing a nonuniform surface and spatiotemporal patterns. The applied potential has a strong effect on the rate of the reaction and is easily controllable; it thus serves as a parameter that can be varied to investigate transitions among states.

Surface reaction studies exhibit a certain amount of drift and noise and, of more direct importance to the experiments described here, are done on surfaces that are not perfectly uniform. Surface heterogeneities can, of course, influence the observed patterns [17,22,29]. Nevertheless, the results presented here are reproducible and appear to be due to the dynamics of the system. We carried out each of these experiments several times with the same results. Rotation of the ring has no effect. In addition, we have observed the same patterns on different rings of various sizes, which is another indication that the heterogeneities do not play a major role in the overall dynamics. The heterogeneities and noise, however, do contribute to the small-scale imperfections in the patterns.

There is another factor that can influence patterns on a surface, i.e., the geometry of the cell including the orientation of the working electrode (the ring) and its position relative to the counter- and reference electrodes. As noted above, in the present experiments the reference electrode is located in the horizontal plane of the working electrode, just outside the radius of the epoxy. Thus there is a slight asymmetry in the apparatus. The effect of this asymmetry in the present system is not completely understood; however, as seen in the Results section the base state pattern is to the accuracy of the experiments O(2) symmetric and thus the effect appears to be small. Since geometry is important in affecting the degree of coupling among reacting sites, it is likely that different sequences of patterns could be obtained by making substantial alterations in the system, such as by varying the height or radial position of the reference electrode, by moving the position of the counterelectrode, etc.; large changes in these quantities can even destroy the O(2) symmetry of the base case. It was not our intention here to investigate all effects of changes in geometry but rather to study the bifurcation structure starting from a base state that was O(2) symmetric.

The sequence of patterns consisting of a p_1 relaxation oscillation with O(2) symmetry, a p_2 oscillation, a symmetry broken p_2 oscillation, and a p_4 oscillation appears to arise from the dynamics of the electrochemical system.

ACKNOWLEDGMENT

The authors gratefully acknowledge the support of the National Science Foundation.

[1] A. S. Mikhailov, *Foundation of Synergetics I: Distributed Active Systems* (Springer-Verlag, Berlin, 1994).
[2] A. Palacios, G. H. Gunaratne, and M. Gorman, Chaos **7**, 463 (1997).
[3] A. Bayliss and B. J. Matkowsky, SIAM (Soc. Ind. Appl. Math.) J. Appl. Math. **52**, 396 (1992).
[4] U. Middya, D. Luss, and M. Sheintuch, J. Chem. Phys. **100**, 3568 (1994).
[5] M. A. Liauw *et al.*, AIChE J. **43**, 1519 (1997).
[6] M. D. Graham *et al.*, Science **264**, 80 (1994).
[7] A. T. Winfree, Chaos **1**, 303 (1991).
[8] J. Maselko, J. S. Reckley, and K. Showalter, J. Phys. Chem. **93**, 2774 (1989).
[9] A. Toth, V. Gaspar, and K. Showalter, J. Phys. Chem. **98**, 522 (1994).
[10] K. I. Agladze *et al.*, Z. Phys. Chem. **173**, 79 (1991).
[11] W. Y. Tam *et al.*, Phys. Rev. Lett. **61**, 2163 (1988).
[12] J. L. Hudson and T. T. Tsotsis, Chem. Eng. Sci. **49**, 1493 (1994).
[13] K. Krischer, in *Modern Aspects of Electrochemistry*, edited by B. E. Conway, O. M. Bockris, and R. E. White (Kluwer/Plenum, New York, 1999), Vol. 32, p. 1.
[14] P. Grauel *et al.*, J. Phys. Chem. B **102**, 10 264 (1998).
[15] J. Christoph *et al.*, J. Chem. Phys. **110**, 8614 (1999).
[16] P. Strasser *et al.*, J. Phys. Chem. A **104**, 1854 (2000).
[17] R. D. Otterstedt *et al.*, Chem. Eng. Sci. **54**, 1221 (1999).
[18] R. D. Otterstedt *et al.*, J. Chem. Soc., Faraday Trans. **92**, 2933 (1996).
[19] Z. Fei, B. J. Green, and J. L. Hudson, J. Phys. Chem. **103**, 2178 (1999).
[20] A. Pigeaud and H. B. Kirkpatrick, Corrosion (Houston) **25**, 209 (1969).
[21] J. L. Hudson *et al.*, Phys. Lett. A **179**, 355 (1993).
[22] J. C. Sayer and J. L. Hudson, Ind. Eng. Chem. Res. **34**, 3246 (1995).
[23] M. Golubitsky, I. Stewart, and D. G. Schaeffer, *Singularities and Groups in Bifurcation Theory* (Springer, New York, 1988).
[24] J. L. Lumley, *The Structure of Inhomogeneous Turbulent Flows, Atmosphere Turbulence and Radio Propagation* (Nauka, Moskow, 1967).
[25] L. Sirovich and C. H. Sirovich, Contemp. Math. **99**, 277 (1989).
[26] J. W. Swift and K. Wiesenfeld, Phys. Rev. Lett. **52**, 705 (1984).
[27] B. Fiedler, *Global Bifurcation of Periodic Solutions with Symmetry* (Springer, Berlin, 1988).
[28] I. Waller and R. Kapral, Phys. Lett. **105A**, 163 (1984).
[29] M. A. Liauw, J. Ning, and D. Luss, J. Chem. Phys. **104**, 5657 (1996).